NEOPLASIA
www.neoplasia.com

Volume 18 Number 10 October 2016 pp. 626–635 626

ASPL-TFE3 Oncoprotein Regulates Cell Cycle Progression and Induces Cellular Senescence by Up-Regulating p21

Naoko Ishiguro* **and Haruhiko Yoshida†**

*Department of Pathobiological Science and Technology, Faculty of Medicine, Tottori University, 86 Nishimachi, Yonago, Tottori 683-8503, Japan; †Department of Pathology, Yonago Medical Center, 4-17-1 Kuzumo, Yonago, Tottori 683-0006, Japan

Abstract

Alveolar soft part sarcoma is an extremely rare soft tissue sarcoma with poor prognosis. It is characterized by the unbalanced recurrent chromosomal translocation der(17)t(X;17)(p11;q25), resulting in the generation of an ASPL-TFE3 fusion gene. ASPL-TFE3 oncoprotein functions as an aberrant transcriptional factor and is considered to play a crucial role in the tumorigenesis of alveolar soft part sarcoma. However, the underlying molecular mechanisms are poorly understood. In this study, we identified p21 ($p21^{WAF1/CIP1}$) as a direct transcriptional target of ASPL-TFE3. Ectopic ASPL-TFE3 expression in 293 cells resulted in cell cycle arrest and significant increases in protein and mRNA levels of p21. ASPL-TFE3 activated p21 expression in a p53-independent manner through direct transcriptional interactions with the p21 promoter region. When ASPL-TFE3 was expressed in human bone marrow–derived mesenchymal stem cells in a tetracycline-inducible manner, we observed the up-regulation of p21 expression and the induction of senescence-associated β-galactosidase activity. Suppression of p21 significantly decreased the induction of ASPL-TFE3-mediated cellular senescence. Furthermore, ASPL-TFE3 expression in mesenchymal stem cells resulted in a significant up-regulation of proinflammatory cytokines associated with senescence-associated secretory phenotype (SASP). These results show that ASPL-TFE3 regulates cell cycle progression and induces cellular senescence by up-regulating p21 expression. In addition, our data suggest a potential mechanism by which ASPL-TFE3-induced senescence may play a role in tumorigenesis by inducing SASP, which could promote the protumorigenic microenvironment.

Neoplasia (2016) 18, 626–635

Introduction

Alveolar soft part sarcoma (ASPS) is an extremely rare sarcoma with unclear origins, comprising 0.5% to 1.0% of all soft tissue sarcomas [1]. Although ASPS typically presents as a slow-growing tumor, its overall survival rate is poor because of chemoresistance and the high incidence of pulmonary and brain metastases during the early stages of this disease [2–4]. Moreover, almost all cases of ASPS have the unbalanced recurrent chromosomal translocation der(17)t(X;17)(p11;q25), which results in generation of the ASPL-TFE3 (also known as ASPSCR1-TFE3) fusion gene [5]. Because the ASPL gene is joined in frame with either the third (type 1) or fourth (type 2) exon of TFE3, two types of fusion transcripts have been identified [5].

TFE3 belongs to the microphthalmia transcription factor-transcription factor E (MiTF-TFE) basic helix–loop-helix leucine zipper transcription factor family, which binds to the E-box DNA consensus sequence CANNTG [6,7]. In a subset of renal cell carcinomas with the translocation Xp11.2, TFE3 fuses with PRCC, CLTC, PSF, NonO, PARP14, LUC7L3, KHSRP, and DVL2, resulting in the expression of PRCC-TFE3, CLTC-TFE3, PSF-TFE3, NonO-TFE3, PARP14-TFE3, LUC7L3-TFE3, KHSRP-TFE3, and DVL2-TFE3 fusion oncogenes, respectively [8–14]. In addition, ASPL-TFE3-positive

Abbreviations: ASPS, alveolar soft part sarcoma; ChIP, chromatin immunoprecipitation; FACS, fluorescence-activated cell sorting; MSCs, mesenchymal stem cells; OIS, oncogene-induced senescence; SA-β-gal, senescence-associated β-galactosidase; SASP, senescence-associated secretory phenotype

Address all correspondence to: Naoko Ishiguro, PhD, Department of Pathobiological Science and Technology, Faculty of Medicine, Tottori University, 86 Nishimachi, Yonago, Tottori 683-8503, Japan.
E-mail: guroko@med.tottori-u.ac.jp

Received 5 July 2016; Revised 5 August 2016; Accepted 11 August 2016

1476-5586
http://dx.doi.org/10.1016/j.neo.2016.08.001

renal cell tumors have also been reported [15]. The cellular roles of ASPL have only been partially characterized, but the mouse homolog TUG is a tethering protein that forces the retention of GLUT4-containing vesicles in the cytoplasm in the absence of insulin [16].

The ASPL-TFE3 fusion gene retains the DNA binding and activation domain of TFE3, whereas the N-terminal region of TFE3 is replaced with ASPL sequences [5]. The ASPL-TFE3 oncoprotein is believed to play crucial roles in the progression of ASPS. ASPL-TFE3 functions as an aberrant transcriptional factor and induces the inappropriate up-regulation of various molecules that contribute to the pathogenesis and progression of ASPS [17]. Indeed, several TFE3 fusion oncoproteins, including ASPL-TFE3, up-regulate the Met receptor tyrosine kinase gene and induce oncogenic phenotypes such as uncontrolled cell proliferation, invasion, and metastasis [18]. However, the molecular roles of ASPL-TFE3 are poorly understood.

Deregulated cell proliferation is critical to tumor formation and progression. Because TFE3 plays roles in the regulation of cell growth [19–21], we hypothesized that ASPL-TFE3 may affect the proliferation of tumor cells by inducing inappropriate expression of cell cycle regulatory proteins. Therefore, we investigated the effects of ASPL-TFE3 on the cell cycle machinery. In this paper, we report that ASPL-TFE3 affected the cell cycle machinery by the direct transcriptional up-regulation of p21. In addition, we reveal that the expression of ASPL-TFE3 in mesenchymal stem cells (MSCs) induced p21-mediated cellular senescence and increased the mRNA level of proinflammatory cytokines.

Materials and Methods

Cells

HeLa human cervical carcinoma cells, 293 human embryonic kidney cells, KATO III human gastric cancer cells, and UE7T-13 human bone marrow-derived MSCs, which were immortalized using retroviruses expressing human papillomavirus protein E7 and human telomerase catalytic subunit (hTERT) [22], were obtained from Health Science Research Resource Bank (Osaka, Japan). Cells were maintained under 5% CO_2 at 37°C in Dulbecco's modified Eagle's medium (Nissui, Tokyo, Japan) containing 10% fetal bovine serum.

Tissue Sample

Frozen tissue was obtained from a patient who underwent surgical treatment for ASPS. Written informed consent was obtained for tissue to be used in research. This study was approved by the Ethics Committee of Tottori University.

Cloning and Reverse Transcription Polymerase Chain Reaction

Total RNA was isolated from frozen tissue of ASPS patient using ISOGEN (Nippon GENE, Tokyo, Japan) according to the manufacturer's instructions and a cDNA clone encoding human ASPL-TFE3 was subsequently amplified by reverse transcription polymerase chain reaction (RT-PCR) using a Takara PrimeScript High Fidelity RT-PCR kit (Takara, Otsu, Japan) with the following primers: forward, 5′-AAGCTTCACCATGGCGGCCCCGG CAGGC-3′ (including HindIII site and Kozak sequence), and reverse, 5′-TCACTTGTCGTCATCGTCTTTGTAGTCGGA CTCCTCTTCCATGCT-3′ (including FLAG epitope tag sequence and STOP codon). Amplified fragments were inserted into the pGeMT-easy vector (Promega, Madison, WI) and DNA was sequenced using ABI PRISM (Applied Biosystems, Foster City, CA). DNA sequencing confirmed the identity of the type I fusion gene of ASPL-TFE3. Subsequently, ASPL-TFE3 cDNA was digested using HindIII and NotI and inserted into the tetracycline-inducible expression vector pcDNA4/TO (Invitrogen, Carlsbad, CA) to produce pcDNA/TO-AT.

Transfection and Selection of Clones

For the tetracycline-regulated system (T-Rex system; Invitrogen), 293 and UE7T-13 cells were transfected with pcDNA6/TR (Invitrogen) and either empty pcDNA4/TO vector or pcDNA/TO-AT using FuGENE HD transfection reagent (Roche, Mannheim, Germany), according to the manufacturer's instructions, and these were designated 293/TR-Vec, 293/TR-AT, UE7T/TR-Vec, and UE7T/TR-AT cells, respectively. After 24 h, cells were placed in media containing 5 μg/ml blasticidin (Invitrogen) and 125 μg/ml Zeocin (Invitrogen), and drug-resistant colonies were isolated. Tetracycline (1 μg/ml; Invitrogen) was added to the growth media to induce of ASPL-TFE3 (tested by RT-PCR and western blotting).

Cell Growth Assay

293/TR-AT and UE7T/TR-AT cells were seeded at densities of 1×10^5 and 2×10^4 cells per well, respectively, in 6 well plates. Tetracycline or phosphate buffered saline (PBS) was added to the media and cells were cultured for designated times. Subsequently, cells were trypsinized and counted using a trypan blue dye exclusion test.

Fluorescence-Activated Cell Sorting Analysis

Cells were trypsinized, harvested, and fixed at −20°C in 70% ethanol for at least overnight. Fixed cells were stained with 1 ml of propidium iodide (PI) solution (0.05% NP-40, 50 μg/ml propidium iodide, and 10 μg/ml RNase A) for at least 2 h at 4°C. Stained cells were analyzed using an EPICS ALTRA flow cytometer (Beckman Coulter, Brea, CA).

Western Blot

Cells were suspended in lysis buffer (0.1% SDS, 40 mM Tris–HCl (pH 7.4), 1% Nonidet P-40, 0.5% sodium deoxycholate, 150 mM NaCl, 4 mM EDTA, 1 mM phenylmethylsulfonyl fluoride, 5 μg/ml aprotinin, 1 μg/ml leupeptin), and were then centrifuged. Lysate samples containing 10 to 20 μg of protein were subjected to SDS-polyacrylamide gel electrophoresis and were then transferred to polyvinylidene difluoride (PVDF) membranes (Millipore, Bedford, MA). PVDF membranes were then incubated overnight at 4°C with primary antibodies and signals were detected using Pierce Western Blotting Substrate (Thermo Scientific, Rockford, IL) according to the manufacturer's instructions. Antibodies against p21, p27, p16, and cyclin dependent kinase (Cdk) 2 were obtained from BD Transduction Laboratories (Franklin Lakes, NJ). Antibodies against FLAG and actin were purchased from Sigma (St Louis, MO). Rb antibody was purchased from Santa Cruz Biotechnology (Santa Cruz, CA) and Cdk4 antibody was obtained from Epitomics (Burlingame, CA). Phosphorylated-Rb (Ser807/811) antibody was purchased from Cell Signaling Technology (Beverly, MA).

Plasmids

The p21 promoter (−2264 to +11 base pairs) was obtained from the DNA Bank, RIKEN BioResource Center (Ibaraki, Japan) and was subcloned into the pGV-B2 vector (Toyo Ink, Tokyo, Japan).

Luciferase Reporter Assay

Cells were plated on 35-mm culture dishes at a density of 2×10^5 per dish. On the next day, the cells were transfected with 0.5 μg of the

luciferase reporter plasmid, a total of 0.5 μg of expression plasmids, and 0.75 μg of the pSV-β-gal vector (Promega) as a reference using FuGENE HD reagent (Roche). After 24 h, cells were lysed and luciferase activity was measured using a Luciferase Assay System (Promega). The activity of firefly luciferase was normalized with the β-galactosidase Enzyme Assay System (Promega).

Chromatin Immunoprecipitation Assays

Chromatin immunoprecipitation (ChIP) assays were performed using ChIP-IT Express Kits (Active Motif, Carlsbad, CA) according to the manufacturer's instructions. Briefly, cells were fixed with 1% formaldehyde for 10 min at room temperature. After lysis, nuclei were isolated using a Dounce homogenizer and were digested in enzymatic shearing cocktail for 10 min. Chromatin isolates were then incubated overnight with antibodies against FLAG (Sigma) or mouse IgG (negative control) and protein G magnetic beads at 4°C with gentle agitation. Subsequently, the beads were collected and washed, and chromatin–protein complexes were eluted. Cross-linking was then reversed by incubation for 15 min at 95°C and purified DNA was subjected to PCR amplification using the primers 5′-TGTTTCAGG CACAGAAAGGAGGCA-3′ and 5′-AAATCCCTGTGGTTGCAG CAGCTT-3′ for the −1239 to −806 bp region of the p21 promoter.

Real-Time Reverse Transcription Polymerase Chain Reaction

Total RNA was isolated from cells using RNeasy mini kits (Qiagen, Hilden, Germany), and first strand cDNA was synthesized from 500 ng of total RNA using PrimeScript RT Reagent Kits (Takara) according to the manufacturer's instructions. Subsequently, cDNA was subjected to real-time PCR using Express qPCR SuperMix (Invitrogen) or GoTaq Probe qPCR master mix (Promega). The primers used were as follows: $p21^{WAF/CIP1}$, 5′-TCACTGTCTTGTACCCTTGTGC-3′ and 5′-GGCGTTTGGAGTGGTAGAAA-3′; IL1A, 5′-AACCAGTG CTGCTGAAGGA-3′ and 5′-TTCTTAGTGCCGTGAGTTTCC-3′; IL1B, 5′-AAAGCTTGGTGATGTCTGGTC-3′ and 5′-GGACAT GGAGAACACCACTTG-3′; IL6, 5′-TTCTCCACAA GCGCCTTC-3′ and 5′-GGAATCTTCTCCTGGGGGTA-3′; IL8, 5′-GAGCACTCCATAAGGCACAAA-3′ and 5′-ATGG TTCCTTCCGGTGGT-3′; beta-actin, 5′-GCACCCAGCACAATG AAGA-3′ and 5′-CGATCCACACGGAGTACTTG-3′. Gene expression was normalized to that of beta-actin, and data were analyzed using the comparative Ct method.

Senescence-Associated β-Galactosidase Staining

Cells were fixed by incubation in 2% formaldehyde/0.2% glutaraldehyde/PBS for 5 min at room temperature and were then stained with X-gal solution (1 mg/mL X-gal, 5 mM $K_3Fe[CN]_6$, 5 mM $K_4Fe[CN]_6$, 2 mM $MgCl_2$ in 40 mM citric acid/Na phosphate buffer at pH 6.0) at 37°C for 24 h.

RNA Interference

Cells were seeded in 12-well plates at 5×10^4 per well and were transfected with 150 ng siRNAs using HiPerFect reagent (Qiagen) according to the manufacturer's instructions. The two human p21 siRNAs were purchased from Sigma Genosys (Sigma Genosys Japan, Hokkaido, Japan) and the control siRNA was obtained from Qiagen. The corresponding p21 siRNA sequences were GAUGGAA CUUCGACUUUGUUU (sense-1), ACAAAGUCGAAGUUCCA UCUU (antisense-1), CAGACCAGCAUGACAGAUUUU (sense-2), and AAUCUGUCAUGCUGGUCUGUU (antisense-2).

Statistical Analysis

The statistical significances were determined by Student's *t*-test and *P* values <.05 were considered to be statistically significant.

Results

ASPL-TFE3 Induces Cell Cycle Arrest in 293 Cells

We established 293 cells that express ASPL-TFE3 in a tetracycline-inducible manner, and designated them as 293/TR-AT cells. Induction of ASPL-TFE3 expression by tetracycline addition was confirmed by immunoblotting (Figure 1*A*). To determine whether ASPL-TFE3 expression affects cell proliferation, 293/TR-AT cells were cultured with tetracycline and their proliferation was evaluated. As shown in Figure. 1*B*, the induction of ASPL-TFE3 expression in 293/TR-AT cells inhibited cell proliferation. Fluorescence-activated cell sorting (FACS) analysis revealed that ASPL-TFE3 expression resulted in an increase in the population of cells in the G_0/G_1 phase, with a concomitant decrease in the number of cells in the S phase (Figure 1*C*), suggesting that ASPL-TFE3 induces growth arrest in 293 cells.

ASPL-TFE3 Increases p21 mRNA and Protein Expression

Because cell cycle progression is regulated by complexes of cell cycle regulatory proteins that include cyclins, Cdk, and Cdk inhibitors, we analyzed the expression of cell cycle regulatory proteins in 293/TR-AT cells following tetracycline treatment. The induction of ASPL-TFE3 expression resulted in an increase in protein level of the Cdk inhibitor p21 [23,24], whereas the expression levels of other cell cycle regulatory proteins, including p27, p16, p53, Cdk2, and Cdk4, showed no remarkable changes (Figure 2*A*). Up-regulated p21 protein expression was detectable as early as 2 h after tetracycline treatment, in parallel with ASPL-TFE3 protein expression (Supplementary Figure 1). We further investigated the phosphorylation level of Rb, which plays a key role during the transition from G_0/G_1 to S phases [25,26], and observed a decrease in its phosphorylation level after tetracycline treatment (Figure 2*A*). These findings indicate that ASPL-TFE3 expression increases p21 protein level and decreases the phosphorylation level of Rb, resulting in growth arrest of 293 cells.

To further confirm ASPL-TFE3-induced up-regulation of p21, we transiently transfected HeLa cells with ASPL-TFE3 and subsequently observed an increase in p21 protein expression (Figure 2*B*). Moreover, in real-time quantitative RT-PCR analyses, the induction of ASPL-TFE3 expression in 293/TR-AT cells resulted in an approximately 5-fold increase in p21 mRNA level (Figure 2*C*).

p21 is a Direct Target Gene of ASPL-TFE3

Because the ASPL-TFE3 fusion oncoprotein functions as an aberrant transcription factor, we investigated whether ASPL-TFE3 activates the p21 gene promoter using luciferase reporter assays of the full-length human p21 promoter. Cotransfection of the ASPL-TFE3 expression vector and the reporter vector in HeLa cells caused a marked increase in luciferase activity compared with that following transfection with the control empty vector (Figure 3*A*). Because p53 is a well-known inducer of p21 [23], we determined whether p53 is required for activation of the p21 promoter by ASPL-TFE3, and found that transiently expressed ASPL-TFE3 activated the p21 gene promoter in p53-deficient ($p53^{-/-}$) KATO III cells (Figure 3*A*). We next investigated the binding of ASPL-TFE3 to the p21 promoter using ChIP assays with an anti-FLAG antibody. After 24 h of incubation with tetracycline, DNA–protein complexes were

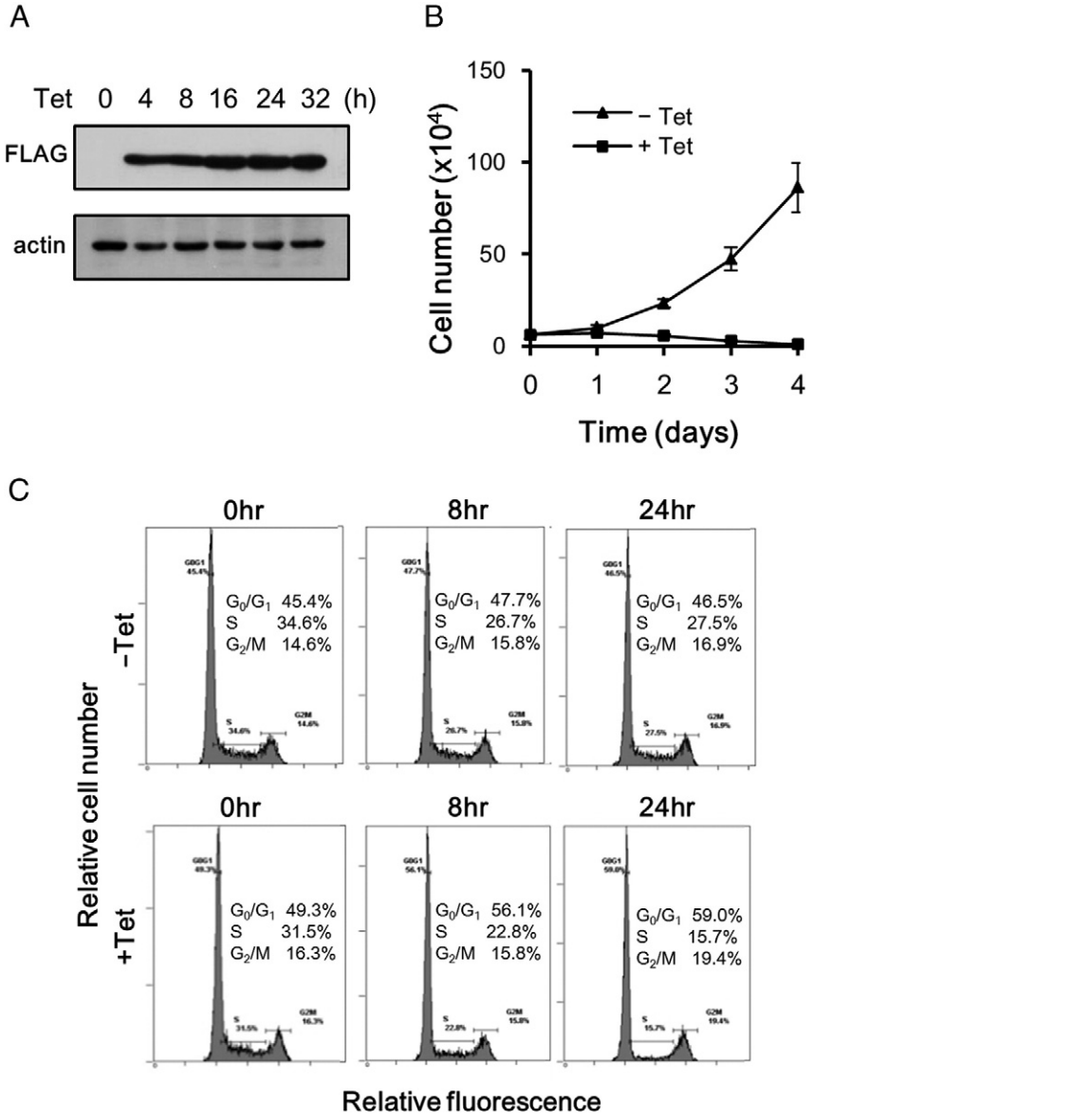

Figure 1. Effects of ASPL-TFE3 on cell proliferation and cell cycle progression. (A) 293/TR-AT cells were cultured in the presence of tetracycline for the indicated times and were then subjected to immunoblot analyses using the indicated antibodies. The expression levels of ASPL-TFE3 were examined using immunoblotting with anti-FLAG antibody. (B) 293/TR-AT cells were cultured in the presence or absence of tetracycline (+ or − Tet) for the indicated times and the cell numbers were determined. Experiments were performed twice with triplicate determinations for each time point. Data are presented as mean ± standard deviation (SD). (C) Cell cycle distributions of 293/TR-AT cells were analyzed using FACS. 293/TR-AT cells were cultured in the presence or absence of tetracycline (+ or − Tet) for the indicated times and were then stained with PI for FACS analyses.

immunoprecipitated from 293/TR-AT cells and direct binding of the FLAG-tagged ASPL-TFE3 with the endogenous p21 promoter was observed (Figure 3*B*). Collectively, these results indicate that ASPL-TFE3 directly binds to the p21 promoter and modulates its transcriptional activity independent of p53.

ASPL-TFE3 Induces Cellular Senescence in Human Mesenchymal Stem Cells

Various cellular stresses, including DNA damage and oncogene expression, cause irreversible cell cycle arrest termed premature senescence [27]. Besides its effect on cell cycle progression, p21 has been reported to induce cellular senescence [27,28]. Thus, we hypothesized that ASPL-TFE3-mediated up-regulation of p21 may contribute to the induction of cellular senescence. To investigate this possibility, we assessed the activity of senescence-associated β-galactosidase (SA-β-gal), a well-defined senescence biomarker [29], in 293/TR-AT cells. However, the proportions of SA-β-gal-positive cells were independent of ASPL-TFE3 expression (data not shown).

Oncogene expression induces premature senescence termed oncogene-induced senescence (OIS) in certain cell types, including primary fibroblasts and progenitor/stem cells [27,30]. Furthermore, recent studies have reported that the expression of sarcoma-associated fusion oncogenes in MSCs can lead to the development of tumors resembling sarcomas [31–34], suggesting that MSCs are a potential model for analyzing the pathogenesis of sarcomas with specific fusion

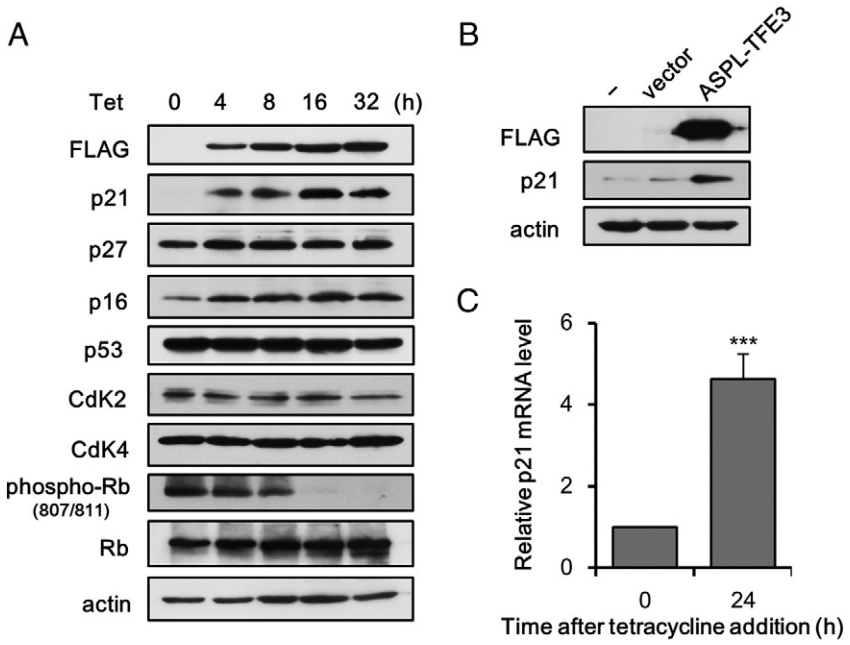

Figure 2. ASPL-TFE3 up-regulates p21. (A) 293/TR-AT cells were cultured in the presence of tetracycline for the indicated times and were then subjected to immunoblot analyses using the indicated antibodies. (B) HeLa cells were transiently transfected with either the vector control or the ASPL-TFE3 expression vector and were incubated for 24 h. Cell lysates were then subjected to immunoblotting using antibodies against FLAG, p21, and actin. (C) p21 mRNA levels were determined using real-time quantitative PCR in 293/TR-AT cells cultured in the presence of tetracycline for 0 or 24 h. Relative p21 expression was analyzed using quantitative PCR and gene expression data were normalized to those for beta-actin. Data are presented as fold changes in mRNA levels relative to no treatment (0 h) from three independent experiments. Error bars show SD; ***$P < .005$.

proteins. Therefore, we established a tetracycline-inducible system for ASPL-TFE3 in UE7T-13 human bone marrow-derived MSCs (UE7T/TR-AT cells) and confirmed the induction of ASPL-TFE3 expression by tetracycline addition using immunoblotting (Figure 4*A*). As shown in Figure 4*B*, the addition of tetracycline resulted in suppression of the proliferation of UE7T/TR-AT cells. We next examined the expression of cell cycle regulators in UE7T/TR-AT cells and found that the induction of ASPL-TFE3 expression markedly increased p21 protein expression, whereas the expression of p53, p16, and p27 showed no remarkable changes (Figure 4*C*). To determine whether

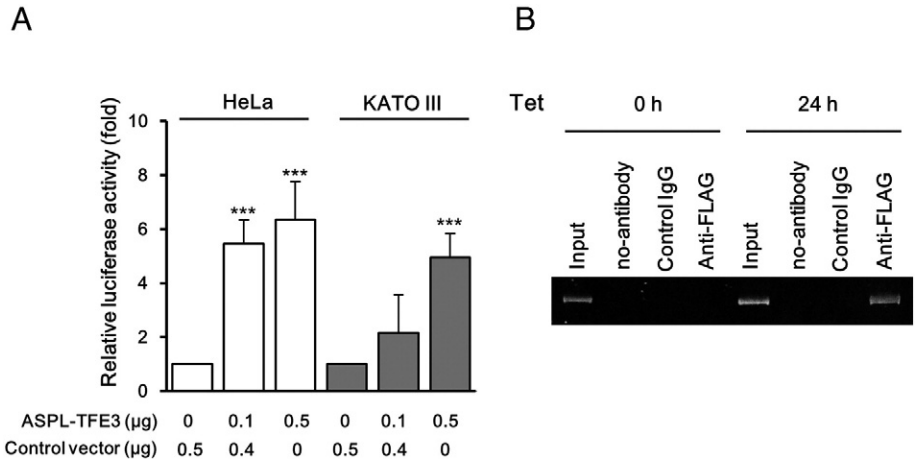

Figure 3. p21 is a direct target of ASPL-TFE3. (A) Luciferase reporter plasmids containing the p21 promoter sequence were co-transfected into HeLa cells or p53-deficient KATO III cells with the indicated amount of empty vector and/or expression vector for ASPL-TFE3. Cells were harvested 24 h after transfection and luciferase activity was assayed. Data are presented as the fold changes in luciferase activity relative to that in cells transfected with the control vector. Data are presented as mean ± SD of at least three independent experiments. ***$P < .005$. (B) ChIP analysis of 293/TR-AT cells using PCR primers specific for the p21 promoter. Chromatin was isolated from 293/TR-AT cells cultured in the presence of tetracycline for 0 or 24 h, immunoprecipitated with anti-FLAG antibody or control mouse IgG, followed by analysis by PCR amplification. Input represents the enzymatically sheared chromatin prior to immunoprecipitation.

ASPL-TFE3 expression induces cellular senescence, we performed SA-β-gal staining in UE7T/TR-AT cells following tetracycline treatment (Figure 4*D*). ASPL-TFE3 expression in UE7T/TR-AT cells resulted in an increase in the percentage of SA-β-gal-positive cells from 2% at 0 h to 20% at 24 h and 32% at 48 h after tetracycline treatment (Figure 4*E*). The proportions of SA-β-gal-positive cells were increased by 46% at 4 days after tetracycline treatment, followed by a slight decrease to 35% at 8 days after tetracycline treatment (Supplementary Figure 2).

p21 is a Mediator of ASPL-TFE3-Induced Senescence

To determine whether p21 contributes to the induction of cellular senescence by ASPL-TFE3, we suppressed p21 expression using p21 siRNAs (p21–1 and p21–2) in tetracycline-treated UE7T/TR-AT cells (Figure 5*A*). UE7T/TR-AT cells were transfected with either control siRNA or p21 siRNAs, and SA-β-gal staining was performed (Figure 5*B*). After 48 h of incubation with tetracycline, 31% of control siRNA-transfected cells were positive for SA-β-gal staining, whereas the transfection of p21 siRNAs p21–1 and p21–2 decreased the proportions of SA-β-gal-positive cells to 16% and 17%, respectively (Figure 5*C*). These findings indicate that ASPL-TFE3-induced senescence is mediated at least in part by p21 expression.

ASPL-TFE3 Up-Regulates The Expression of Proinflammatory Cytokines

One of the hallmarks of senescent cells is the senescence-associated secretory phenotype (SASP), which influences the microenvironment via the secretion of proinflammatory cytokines and growth factors [35,36]. Senescent cells have undergone widespread changes in

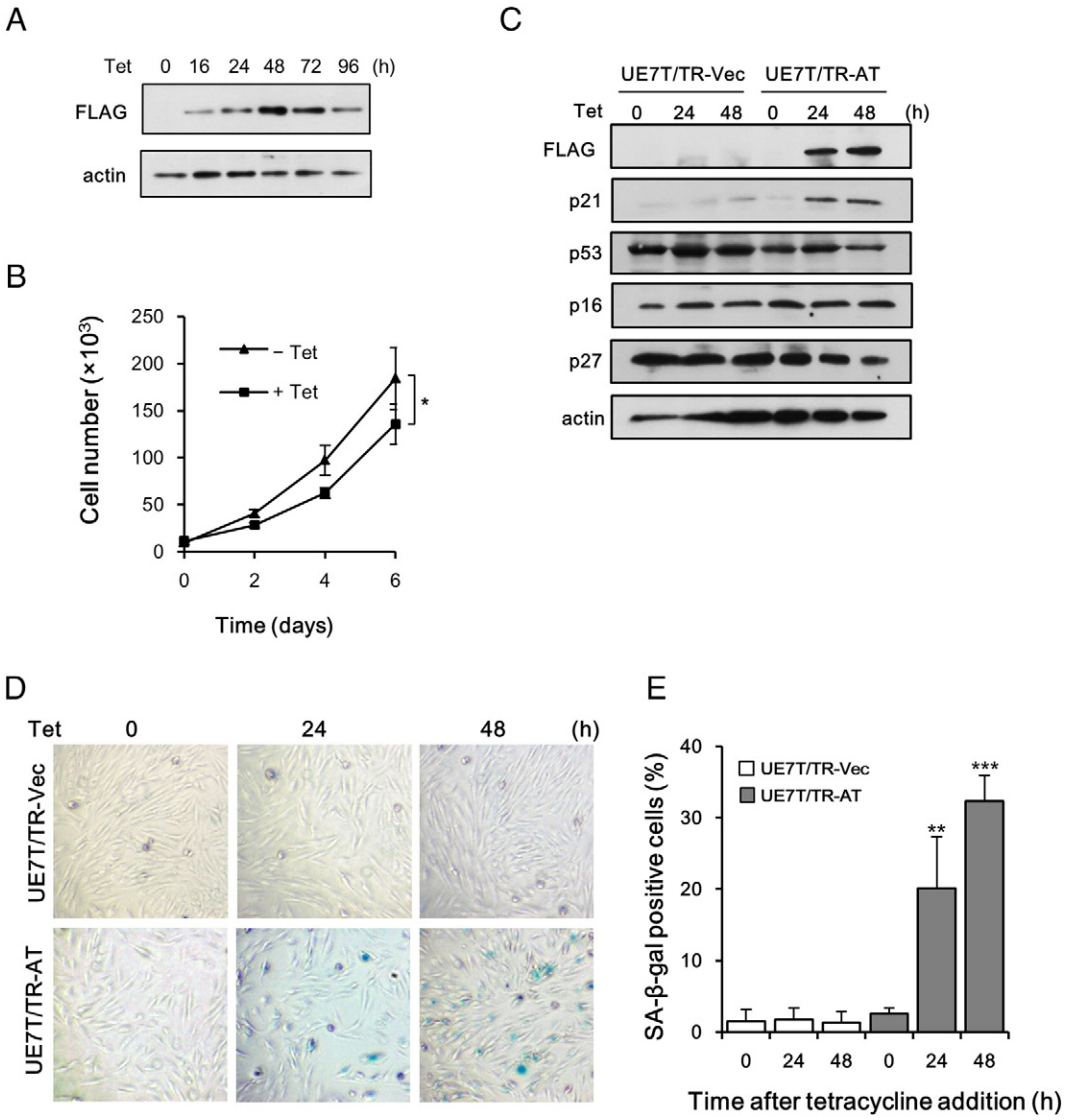

Figure 4. ASPL-TFE3 induces cellular senescence in mesenchymal stem cells. (A) UE7T/TR-AT cells were cultured in the presence of tetracycline for the indicated times and were then subjected to immunoblot analyses using the indicated antibodies. (B) UE7T/TR-AT cells were cultured in the presence or absence of tetracycline (+ or − Tet) for the indicated times and cell numbers were then determined. Experiments were performed twice with triplicate determinations for each time point. Data are presented as mean ± SD. *$P < .05$. (C) UE7T/TR-Vec and UE7T/TR-AT cells were incubated with tetracycline for 0, 24, and 48 h and were then subjected to immunoblotting with the indicated antibodies. (D) SA-β-gal staining was performed in UE7T/TR-Vec and UE7T/TR-AT cells after tetracycline treatment for 0, 24, and 48 h. (E) Proportions of SA-β-gal-positive cells in cultures of UE7T/TR-Vec and UE7T/TR-AT cells were calculated after tetracycline treatment for 0, 24, and 48 h. Data are presented as mean ± SD of three independent experiments. **$P < .01$; ***$P < .005$.

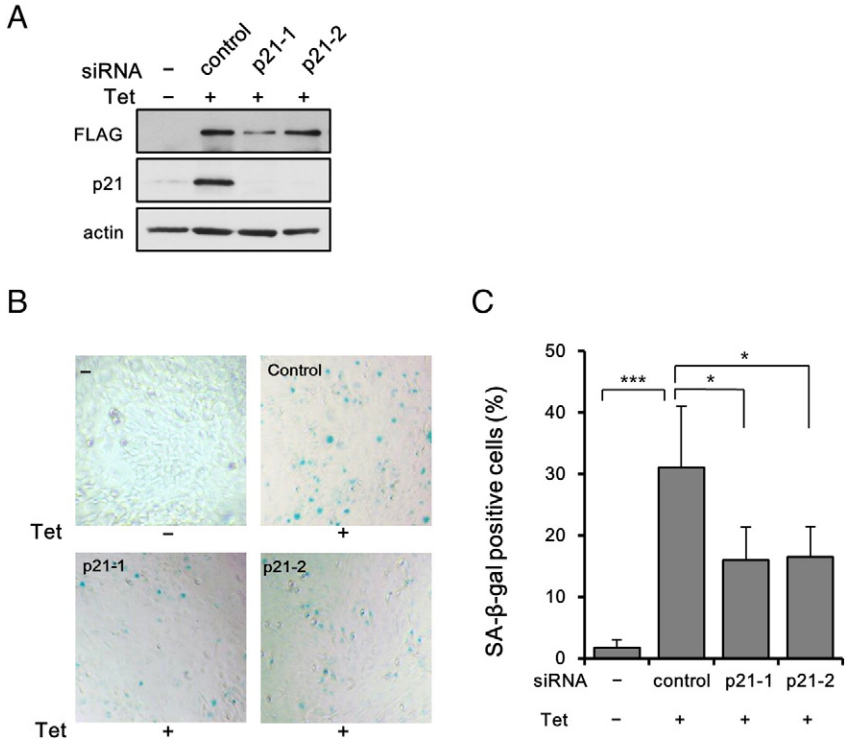

Figure 5. Suppression of p21 reduces ASPL-TFE3-induced senescence. (A) UE7T/TR-AT cells were transfected with either control siRNA or p21 siRNAs (p21–1 and p21–2), and were then cultured in the presence of tetracycline (Tet +) for 48 h. Lysates of untreated UE7T/TR-AT cells (−) or siRNA-transfected cells were subjected to immunoblotting using the indicated antibodies. (B) SA-β-gal staining was performed in untreated UE7T/TR-AT cells (−) or UE7T/TR-AT cells transfected with either control siRNA or p21 siRNAs (p21–1 and p21–2) after tetracycline treatment for 48 h. (C) Proportions of SA-β-gal-positive cells were calculated for all treatment groups. Data are presented as mean ± SD of three independent experiments. *$P < .05$; ***$P < .005$.

protein expression and secretion, ultimately leading to the SASP. Despite the tumor-suppressing role of senescence-associated cell cycle arrest, SASP has been suggested to promote tumorigenesis [36]. Thus, we examined the expression of representative SASP-associated proinflammatory cytokines, including IL1A, IL1B, IL6, and IL8, in tetracycline-treated UE7T/TR-AT cells by quantitative real-time PCR (Figure 6). At 4 days after tetracycline treatment, the expression of IL1A, IL1B, and IL8 was significantly increased compared with that of untreated UE7T/TR-AT cells. In contrast, the expression levels of IL1B, IL6, and IL8 were decreased at 1 day after tetracycline treatment, suggesting that the up-regulation of proinflammatory cytokines is probably not due to direct transcriptional up-regulation by ASPL-TFE3.

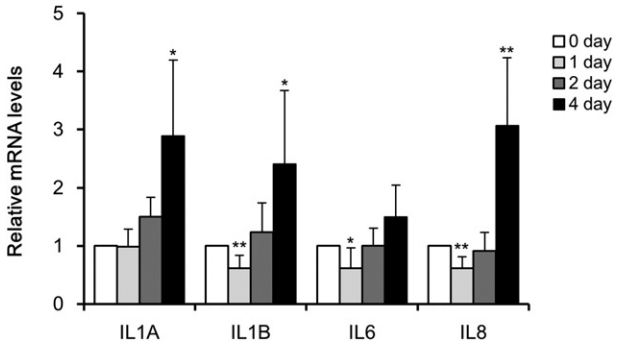

Figure 6. ASPL-TFE3 up-regulates the expression of proinflammatory cytokines. UE7T-TR-AT cells were cultured in the presence of tetracycline for the indicated days, and then the expression of IL1A, IL1B, IL6, and IL8 was analyzed by real-time quantitative PCR. Gene expression data were normalized to those for beta-actin. Data are presented as fold changes in mRNA levels relative to those on day 0 from three independent experiments. Error bars show SD; *$P < .05$; **$P < .01$.

Discussion

The presence of the translocation t(X;17)(p11;q25) in almost all ASPS cases suggests that the ASPL-TFE3 fusion gene contributes to tumor formation and progression, but the corresponding oncogenic mechanisms are poorly defined. Here, we demonstrate a novel mechanism by which ASPL-TFE3 regulates cell cycle progression and induces cellular senescence by directly up-regulating p21 expression. In addition, we find that ASPL-TFE3 expression in MSCs induced the expression of proinflammatory cytokines associated with the SASP.

Fusion oncogenes that act as transcription factors play critical roles in tumor formation and progression through their transcriptional targets. In this study, we identified p21 as a novel transcriptional target of ASPL-TFE3. Ectopic expression of ASPL-TFE3 in 293 cells resulted in growth arrest and increases in p21 protein and mRNA levels. By luciferase and ChIP assays, we provided evidence that ASPL-TFE3 directly interacts with the p21 promoter region and activates it. Consistent with our results, another TFE3 fusion oncoprotein, PRCCTFE3, which carries the DNA binding domain of TFE3, causes cell cycle delays by transcriptionally up-regulating p21 expression [37]. Thus, TFE3 fusion oncoproteins appear to affect the

cell cycle machinery through a p21-mediated mechanism. It should be noted, however, that in clinical samples of Xp11 translocation renal cell carcinomas, p21 protein overexpression has not been observed consistently [38].

In this study, we show for the first time that ASPL-TFE3 expression can provoke cellular senescence. The expression of activated oncogenes, such as Ras and fusion oncogenes, induces OIS through activation of the p53/p21 pathway and/or p16 pathway [27,28]. Our data revealed that ASPL-TFE3 expression in MSCs induced some hallmarks of OIS, including the induction of SA-β-gal activity and increased p21 expression. The expression of ASPL-TFE3 in MSCs increased the protein level of p21 while not affecting the expression of p16, p53, and p27, suggesting that p21 is an important mediator of ASPL-TFE3-induced senescence. Given that ASPL-TFE3 activated the p21 promoter in p53-deficient Kato III cells, ASPL-TFE3 appears to induce senescence in a p53-independent manner.

The significance of p21 in ASPL-TFE3-induced senescence was further supported by the observation that the proportion of SA-β-gal-positive cells was decreased after p21 suppression in ASPL-TFE3-expressing UE7T/TR-AT cells. Nevertheless, p21 suppression did not completely abolish the induction of SA-β-gal expression. Recent studies suggest that OIS is mediated by sequential activation of the p38 MAPK and PI3K/AKT/mTOR pathways [39–41]. Because ASPL-TFE3 activates the MAPK pathway and PI3K/AKT/mTOR pathway by directly up-regulating MET expression [18], additional pathways that include the MAPK and PI3K/AKT/mTOR pathways may also contribute to the ASPL-TFE3-induced senescence.

Our data demonstrate that ASPL-TFE3 expression in MSCs induced cellular senescence, while ASPL-TFE3 expression in 293 cells resulted in growth arrest but failed to induce senescence. These results suggest that the cellular context is important for the molecular roles of ASPL-TFE3. This notion is further supported by evidence that despite harboring the same fusion gene, ASPS is cathepsin K positive, while ASPL-TFE3-positive renal cell carcinoma is cathepsin K negative [42]. The cellular origin of ASPS is currently unclear. However, Goodwin et al. reported that ASPL-TFE3 expression alone, without an additional oncogenic event, is sufficient for invasive sarcomagenesis in mice [43]. Thus, the expression of ASPL-TFE3 in an appropriate cell type may provide clues to understanding the cellular events in ASPS pathogenesis. On the other hand, recent studies have reported that the expression of sarcoma-associated fusion genes, such as EWS-Fli1 and FUS-CHOP, in human MSCs resulted in cellular transformation, implying that MSCs can provide a cellular environment that enables sarcoma-specific fusion proteins to exert their oncogenic potentials [32,44,45]. Gene expression profiling studies of ASPS suggest that ASPSs express genes implicated in myogenic, neurogenic, and stem cell differentiation, further supporting the notion that mesenchymal stem/progenitor cells are appropriate for use as a model for studying the biology of ASPS [46,47]. The issue of whether ASPL-TFE3 can transform human MSCs remains to be clarified, but ASPL-TFE3-expressing MSCs are thought to be a good model for analyzing the cellular events in ASPL-TFE3-associated sarcomagenesis.

Cellular senescence is a tumor-suppressive mechanism that prevents uncontrolled proliferation [48–51]. However, accumulating evidence suggests that senescent cells paradoxically promote tumor progression through the SASP, which can affect their microenvironment via the secretion of proinflammatory cytokines and growth factors [52–54]. Our data revealed that ASPL-TFE3-induced senescence in MSCs was accompanied by an increase in the expression of SASP-associated proinflammatory cytokines. SASP factors have been shown to promote tumor progression by inducing proliferation, epithelial-to-mesenchymal transformation (EMT), and invasion, and promoting angiogenesis [55–57]. Although the exact biological effect of this phenomenon on tumor cell behavior requires further investigation, these observations raise the possibility that ASPL-TFE3-induced senescence can alter the tissue microenvironment by inducing SASP, which can promote malignant phenotypes such as proliferation and invasiveness.

In conclusion, we demonstrate that p21 is a novel transcriptional target of ASPL-TFE3 oncoprotein, and that ASPL-TFE3 affects cell cycle machinery and induces cellular senescence by up-regulating p21 expression. Furthermore, the present work provides a potential mechanism by which ASPL-TFE3-induced senescent cells may promote a protumorigenic microenvironment by secreting proinflammatory cytokines. Since senescence plays an important role in tumor prevention and influences the outcome of cancer therapy [58], knowledge of the molecular mechanisms of ASPL-TFE3-induced senescence may provide clues not only for understanding the oncogenic properties of ASPL-TFE3 but also for developing future therapeutic approaches for ASPS.

Supplementary data to this article can be found online at http://dx.doi.org/10.1016/j.neo.2016.08.001.

Acknowledgements

The authors thank Megumi Asakura for secretarial assistance. This work was supported in part by grants from MEXT KAKENHI (21790352) and JSPS KAKENHI (24790387).

References

[1] Folpe AL and Deyrup AT (2006). Alveolar soft-part sarcoma: a review and update. *J Clin Pathol* **59**, 1127–1132.

[2] Lieberman PH, Brennan MF, Kimmel M, Erlandson RA, Garin-Chesa P, and Flehinger BY (1989). Alveolar soft-part sarcoma. A clinico-pathologic study of half a century. *Cancer* **63**, 1–13.

[3] Portera Jr CA, Ho V, Patel SR, Hunt k, Feig BW, Respondek PM, Yasko AW, Benjamin RS, Pollock RE, and Pisters PW (2001). Alveolar soft part sarcoma: clinical course and patterns of metastasis in 70 patients treated at a single institution. *Cancer* **91**, 585–591.

[4] Ogose A, Yazawa Y, Ueda T, Hotta T, Kawashima H, Hatano H, Morita T, and Japanese Musculoskeletal Oncology Group (2003). Alveolar soft part sarcoma in Japan: multi-institutional study of 57 patients from the Japanese Musculoskeletal Oncology Group. *Oncology* **65**, 7–13.

[5] Ladanyi M, Lui MY, Antonescu CR, Krause-Boehm A, Meindl A, Argani P, Healey JH, Ueda T, Yoshikawa H, and Meloni-Ehrig A, et al (2001). The der(17)t(X;17)(p11;q25) of human alveolar soft part sarcoma fuses the TFE3 transcription factor gene to ASPL, a novel gene at 17q25. *Oncogene* **20**, 48–57.

[6] Beckmann H, Su LK, and Kadesch T (1990). TFE3: a helix–loop-helix protein that activates transcription through the immunoglobulin enhancer muE3 motif. *Genes Dev* **4**, 167–179.

[7] Hemesath TJ, Steingrímsson E, McGill G, Hansen MJ, Vaught J, Hodgkinson CA, Arnheiter H, Copeland NG, Jenkins NA, and Fisher DE (1994). microphthalmia, a critical factor in melanocyte development, defines a discrete transcription factor family. *Genes Dev* **8**, 2770–2780.

[8] Sidhar SK, Clark J, Gill S, Hamoudi R, Crew AJ, Gwilliam R, Ross M, Linehan WM, Birdsall S, and Shipley J, et al (1996). The t(X;1)(p11.2;q21.2) translocation in papillary renal cell carcinoma fuses a novel gene PRCC to the TFE3 transcription factor gene. *Hum Mol Genet* **5**, 1333–1338.

[9] Weterman MA, Wilbrink M, and Geurts van Kessel A (1996). Fusion of the transcription factor TFE3 gene to a novel gene, PRCC, in t(X;1)(p11;q21)–positive papillary renal cell carcinomas. *Proc Natl Acad Sci U S A* **93**, 15294–15298.

[10] Argani P, Lui MY, Couturier J, Bouvier R, Fournet JC, and Ladanyi M (2003). A novel CTCL-TFE3 gene fusion in pediatric renal adenocarcinoma with t(X;17)(p11.2;q23). *Oncogene* **22**, 5374–5378.

[11] Clark J, Lu YJ, Sidhar SK, Parker C, Gill S, Smedley D, Hamoudi R, Linehan WM, Shipley J, and Cooper CD (1997). Fusion of splicing factor genes PSF and Nono (p54 nrb) to the TFE3 gene in papillary renal cell carcinoma. *Oncogene* **15**, 2233–2239.

[12] Huang W, Goldfischer M, Babyeva S, Mao Y, Volyanskyy K, Dimitrova N, Fallon J, and Zhong M (2015). Identification of a novel PARP14-TFE3 gene fusion from 10-year-old FFPE tissue by RNA-seq. *Genes Chromosomes Cancer* **54**, 500–505.

[13] Malouf GG, Su X, Yao H, Gao J, Xiong L, He Q, Compérat E, Couturier J, Molinié V, and Escudier B, et al (2014). Next-generation sequencing of translocation renal cell carcinoma reveals novel RNA splicing partners and frequent mutations of chromatin-remodeling genes. *Clin Cancer Res* **20**, 4129–4140.

[14] Argani P, Zhong M, Reuter VE, Fallon JT, Epstein JI, Netto GJ, and Antonescu CR (2016). TFE3-fusion variant analysis defines specific clinicopathologic associations among Xp11 translocation cancers. *Am J Surg Pathol* **40**, 723–737.

[15] Argani P, Antonescu CR, Illei PB, Lui MY, Timmons CF, Newbury R, Reuter VE, Garvin AJ, Perez-Atayde AR, and Fletcher JA, et al (2001). Primary renal neoplasms with the ASPL-TFE3 gene fusion of alveolar soft part sarcoma: a distinctive tumor entity previously included among renal cell carcinomas of children and adolescents. *Am J Pathol* **159**, 179–192.

[16] Bogan JS, Hendon N, McKee AE, Tsao TS, and Lodish HF (2003). Functional cloning of TUG as a regulator of GLUT4 glucose transporter trafficking. *Nature* **425**, 727–733.

[17] Kobos R, Nagai M, Tsuda M, Merl MY, Saito T, Lae M, Mo Q, Olshen A, Lianoglou S, and Leslie C, et al (2013). Combining integrated genomics and functional genomics to dissect the biology of a cancer-associated, aberrant transcription factor, the ASPSCR1-TFE3 fusion oncoprotein. *J Pathol* **229**, 743–754.

[18] Tsuda M, Davis IJ, Argani P, Shukla N, McGill GG, Nagai M, Saito T, Laé M, Fisher DE, and Ladanyi M (2007). TFE3 fusions activate MET signaling by transcriptional up-regulation, defining another class of tumors as candidates for therapeutic MET inhibition. *Cancer Res* **67**, 919–929.

[19] Giangrande PH, Zhu W, Rempel RE, Laakso N, and Nevins JR (2004). Combinatorial gene control involving E2F and E Box family members. *EMBO J* **23**, 1336–1347.

[20] Giangrande PH, Hallstrom TC, Tunyaplin C, Calame K, and Nevins JR (2003). Identification of E-Box Factor TFE3 as a functional partner for the E2F3 transcription factor. *Mol Cell Biol* **23**, 3707–3720.

[21] Nijman SMB, Hijmans EM, Messaoudi SE, van Dongen MMW, Sardet C, and Bernards R (2006). A functional genetic screen identifies TFE3 as a gene that confers resistance to the anti-proliferative effects of the retinoblastoma protein and transforming growth factor-β. *J Biol Chem* **281**, 21582–21587.

[22] Mori T, Kiyono T, Imabayashi H, Takeda Y, Tsuchiya K, Miyoshi S, Makino H, Matsumoto K, Saito H, and Ogawa S, et al (2005). Combination of hTERT and bmi-1, E6, or E7 induces prolongation of the life span of bone marrow stromal cells from an elderly donor without affecting their neurogenic potential. *Mol Cell Biol* **25**, 5183–5195.

[23] el-Deiry WS, Tokino T, Velculescu VE, Levy DB, Parsons R, Trent JM, Lin D, Mercer WE, Kinzler KW, and Vogelstein B (1993). WAF1, a potential mediator of p53 tumor suppression. *Cell* **75**, 817–825.

[24] Harper JW, Adami GR, Wei N, Keyomarsi K, and Elledge SJ (1993). The p21 Cdk-interacting protein Cip1 is a potent inhibitor of G1 cyclin-dependent kinases. *Cell* **75**, 805–816.

[25] Weintraub SJ, Chow KN, Luo RX, Zhang SH, He S, and Dean DC (1995). Mechanism of active transcriptional repression by the retinoblastoma protein. *Nature* **375**, 812–816.

[26] Weinberg RA (1995). The retinoblastoma protein and cell cycle control. *Cell* **81**, 323–330.

[27] Serrano M, Lin AW, McCurrach ME, Beach D, and Lowe SW (1997). Oncogenic ras provokes premature cell senescence associated with accumulation of p53 and p16(INK4a). *Cell* **88**, 593–602.

[28] Narita M, Nuñez S, Heard E, Narita M, Lin AW, Hearn SA, Spector DL, Hannon GJ, and Lowe SW (2003). Rb-mediated heterochromatin formation and silencing of E2F target genes during cellular senescence. *Cell* **113**, 703–716.

[29] Dimri GP, Lee X, Basile G, Acosta M, Scott G, Roskelley C, Medrano EE, Linskens M, Rubelj I, and Pereira-Smith O, et al (1995). A biomarker that identifies senescent human cells in culture and in aging skin in vivo. *Proc Natl Acad Sci U S A* **92**, 9363–9367.

[30] Wajapeyee N, Wang SZ, Serra RW, Solomon PD, Nagarajan A, Zhu X, and Green MR (2010). Senescence induction in human fibroblasts and hematopoietic progenitors by leukemogenic fusion proteins. *Blood* **115**, 5057–5060.

[31] Cironi L, Provero P, Riggi N, Janiszewska M, Suva D, Suva ML, Kindler V, and Stamenkovic I (2009). Epigenetic features of human mesenchymal stem cells determine their permissiveness for induction of relevant transcriptional changes by SYT-SSX1. *PLoS One* **4**(11), e7904.

[32] Riggi N, Suvà ML, Suvà D, Cironi L, Provero P, Tercier S, Joseph JM, Stehle JC, Baumer K, and Kindler V, et al (2008). EWS-FLI-1 expression triggers a Ewing's sarcoma initiation program in primary human mesenchymal stem cells. *Cancer Res* **68**, 2176–2185.

[33] Riggi N, Cironi L, Provero P, Suvà ML, Stehle JC, Baumer K, Guillou L, and Stamenkovic I (2006). Expression of the FUS-CHOP fusion protein in primary mesenchymal progenitor cells gives rise to a model of myxoid liposarcoma. *Cancer Res* **66**, 7016–7023.

[34] Riggi N, Cironi L, Provero P, Suvà ML, Kaloulis K, Garcia-Echeverria C, Hoffmann F, Trumpp A, and Stamenkovic I (2005). Development of Ewing's sarcoma from primary bone marrow-derived mesenchymal progenitor cells. *Cancer Res* **65**, 11459–11468.

[35] Kuilman T, Michaloglou C, Vredeveld LC, Douma S, van Doorn R, Desmet CJ, Aarden LA, Mooi WJ, and Peeper DS (2008). Oncogene-induced senescence relayed by an interleukin-dependent inflammatory network. *Cell* **133**, 1019–1031.

[36] Coppé JP, Desprez PY, Krtolica A, and Campisi J (2010). The senescence-associated secretory phenotype: the dark side of tumor suppression. *Annu Rev Pathol* **5**, 99–118.

[37] Medendorp K, van Groningen JJ, Vreede L, Hetterschijt L, Brugmans L, van den Hurk WH, and van Kessel AG (2009). The renal cell carcinoma-associated oncogenic fusion protein PRCCTFE3 provokes p21 WAF/CIP1–mediated cell cycle delay. *Exp Cell Res* **315**, 2399–2409.

[38] Argani P, Hicks JBA, De Marzo AM, Albadine R, Illei PB, Ladanyi M, Reuter VE, and Netto GJ (2010). Xp11 translocation renal cell carcinoma (RCC): extended immunohistochemical profile emphasizing novel RCC markers. *Am J Surg Pathol* **34**, 1295–1303.

[39] Wang W, Chen JX, Liao R, Deng Q, Zhou JJ, Huang S, and Sun P (2002). Sequential activation of the MEK-extracellular signal-regulated kinase and MKK3/6-p38 mitogen-activated protein kinase pathways mediates oncogenic ras-induced premature senescence. *Mol Cell Biol* **22**, 3389–3403.

[40] Astle MV, Hannan KM, Ng PY, Lee RS, George AJ, Hsu AK, Haupt Y, Hannan RD, and Pearson RB (2012). AKT induces senescence in human cells via mTORC1 and p53 in the absence of DNA damage: implications for targeting mTOR during malignancy. *Oncogene* **31**, 1949–1962.

[41] Xu Y, Li N, Xiang R, and Sun P (2014). Emerging roles of the p38 MAPK and PI3K/AKT/mTOR pathways in oncogene-induced senescence. *Trends Biochem Sci* **39**, 268–276.

[42] Martignoni G, Gobbo S, Camparo P, Brunelli M, Munari E, Segala D, Pea M, Bonetti F, Illei P, and Netto G, et al (2011). Differential expression of cathepsin K in neoplasms harboring TFE3 gene fusions. *Mod Pathol* **24**, 1313–1319.

[43] Goodwin ML, Jin H, Straessler K, Smith-Fry K, Zhu JF, Monument MJ, Crossmann A, Randall RL, Capeddhi MR, and Jones KB (2014). Modeling alveolar soft part sarcomagenesis in the mouse: a role for lactate in the tumor microenvironment. *Cancer Cell* **26**, 851–862.

[44] Rodriguez R, Tornin J, Suarez C, Astudillo A, Rubio R, Yauk C, Williams A, Rosu-Myles M, Funes JM, and Boshoff C, et al (2013). Expression of FUS-CHOP fusion protein in immortalized/transformed human mesenchymal stem cells drives myxoid liposarcoma formation. *Stem Cells* **31**, 2061–2072.

[45] Rodriguez R, Rubio R, and Menendez P (2012). Modeling sarcomagenesis using multipotent mesenchymal stem cells. *Cell Res* **22**, 62–77.

[46] Stockwin LH, Vistica DT, Kenney S, Schrump DS, Butcher DO, Raffeld M, and Shoemaker RH (2009). Gene expression profiling of alveolar soft-part sarcoma (ASPS). *BMC Cancer* **9**, e22.

[47] Selvarajah S, Pyne S, Chen E, Sompallae R, Ligon AH, Nielsen GP, Dranoff G, Stack E, Loda M, and Flavin R (2014). High-resolution array CGH and gene expression profiling of alveolar soft part sarcoma. *Clin Cancer Res* **20**, 1521–1530.

[48] Braig M, Lee S, Loddenkemper C, Rudolph C, Peters AH, Schlegelberger B, Stein H, Dörken B, Jenuwein T, and Schmitt CA (2005). Oncogene-induced senescence as an initial barrier in lymphoma development. *Nature* **436**, 660–665.

[49] Michaloglou C, Vredeveld LC, Soengas MS, Denoyelle C, Kuilman T, van der Horst CM, Majoor DM, Shay JW, Mooi WJ, and Peeper DS (2005). BRAFE600-associated senescence-like cell cycle arrest of human naevi. *Nature* **436**, 720–724.

[50] Chen Z, Trotman LC, Shaffer D, Lin HK, Dotan ZA, Niki M, Koutcher JA, Scher HI, Ludwig T, and Gerald W, et al (2005). Crucial role of p53-dependent cellular senescence in suppression of Pten-deficient tumorigenesis. *Nature* **436**, 725–730.

[51] Collado M and Serrano M (2010). Senescence in tumours: evidence from mice and humans. *Nat Rev Cancer* **10**, 51–57.

[52] Coppé JP, Patil CK, Rodier F, Sun Y, Muñoz DP, Goldstein J, Nelson PS, Desprez PY, and Campisi J (2008). Senescence-associated secretory phenotypes reveal cell-nonautonomous functions of oncogenic RAS and the p53 tumor suppressor. *PLoS Biol* **6**, 2853–2868.

[53] Lasry A and Ben-Neriah Y (2015). Senescence-associated inflammatory responses: aging and cancer perspectives. *Trends Immunol* **36**, 217–228.

[54] Gorgoulis VG and Halazonetis TD (2010). Oncogene-induced senescence: the bright and dark side of the response. *Curr Opin Cell Biol* **22**, 816–827.

[55] Krtolica A, Parrinello S, Lockett S, Desprez PY, and Campisi J (2001). Senescent fibroblasts promote epithelial cell growth and tumorigenesis: a link between cancer and aging. *Proc Natl Acad Sci U S A* **98**, 12072–12077.

[56] Parrinello S, Coppe JP, Krtolica A, and Campisi J (2005). Stromal-epithelial interactions in aging and cancer: senescent fibroblasts alter epithelial cell differentiation. *J Cell Sci* **118**, 485–496.

[57] Coppé JP, Kauser K, Campisi J, and Beauséjour CM (2006). Secretion of vascular endothelial growth factor by primary human fibroblasts at senescence. *J Biol Chem* **281**, 29568–29574.

[58] Schmitt CA, Fridman JS, Yang M, Lee S, Baranov E, Hoffman RM, and Lowe SW (2002). A senescence program controlled by p53 and p16INK4a contributes to the outcome of cancer therapy. *Cell* **109**, 335–346.